How Different Calculations of the Refractive Index Affect Estimates of the Radiative Forcing Efficiency of Ammonium Sulfate Aerosols

CARYNELISA ERLICK

Fredy and Nadine Herrmann Institute of Earth Sciences, The Hebrew University of Jerusalem, Jerusalem, Israel

JONATHAN P. D. ABBATT

Department of Chemistry, University of Toronto, Toronto, Ontario, Canada

YINON RUDICH

Department of Environmental Sciences and Energy Research, Weizmann Institute of Science, Rehovot, Israel

(Manuscript received 3 November 2010, in final form 14 April 2011)

ABSTRACT

Calculations of the radiative properties of hydrated ammonium sulfate (AS) aerosols often employ the conventional volume mixing rule, in which the refractive indices of AS and water are linearly averaged, weighted by their respective volume fractions in solution, and the real part of the refractive index of pure AS is taken to be 1.52–1.55, based on measurements of dry crystalline AS. However, there are significant differences between the refractive indices of AS–water solutions calculated using the conventional volume mixing rule and empirically derived refractive indices. The authors use a simple model for calculating the direct solar radiative forcing efficiency (RFE; radiative forcing divided by optical depth) of an optically thin layer of aerosols to investigate the magnitude of these differences. The difference between the conventional volume mixing rule and empirically derived refractive indices amounts to a modest difference in the direct solar RFE of AS aerosols at the top of the atmosphere at 0.550-μm wavelength and at relative humidities of 37%–99.9%. Without black carbon, the difference in RFE is up to -0.42 W m^{-2} for relative humidities less than around 66% and up to 0.25 W m^{-2} for relative humidities greater than 66%, whereas with 2% black carbon by volume, the range of difference in RFE is up to -0.59 W m^{-2} for relative humidities less than 66% and up to 0.30 W m^{-2} for relative humidities greater than 66%. Although modest, this difference in RFE may become important when investigating regional aerosol forcing in areas with a high concentration of urban and industrial pollution.

1. Introduction

Ammonium sulfate (AS)–containing aerosols are among the most common aerosols in the troposphere, contributing significantly to direct solar radiative forcing of the climate (e.g., Forster et al. 2007). An important consideration in assessing their direct radiative forcing is their change in size and composition due to uptake of water at different relative humidities, which exhibits a well-known hysteresis pattern. As the relative humidity increases from 0%, a crystalline AS particle remains nearly at its dry size until forming a solution at its deliquescence relative humidity of around 80%. As the relative humidity decreases from 100%, an AS aerosol remains in an aqueous state, becoming a supersaturated solution or metastable liquid, from its deliquescence relative humidity down to a relative humidity of around 35% (the crystallization relative humidity) before recrystallizing (e.g., Tang and Munkelwitz 1994; Tang et al. 1995; Martin et al. 2003; Schlenker et al. 2004; Wang et al. 2008; Mikhailov et al. 2009).

Given their hysteresis behavior, most AS aerosols in the troposphere are likely to be found in the aqueous state rather than in the solid state. Internal mixing with other aerosol components, such as organics, alters the hysteresis curve, sometimes allowing water uptake over an even larger range of relative humidities than the range for pure AS aerosols (e.g., Winkler and Junge 1972; Whitby 1984; Weingartner et al. 2002; Braban and Abbatt 2004;

Corresponding author address: Dr. Carynelisa Erlick, Institute of Earth Sciences, The Hebrew University of Jerusalem, Jerusalem 91904, Israel.
E-mail: caryn@vms.huji.ac.il

DOI: 10.1175/2011JAS3721.1

Marcolli et al. 2004; Marcolli and Krieger 2006; Meyer et al. 2009; Hallquist et al. 2009). Internal mixing with other aerosol components thereby increases the likelihood of AS aerosols being found in the aqueous state.

To calculate the scattering properties of AS aerosols in the aqueous state, electromagnetic mixing rules are often used in conjunction with a Mie scattering algorithm for homogeneous spheres (e.g., Bohren and Huffman 1983). One prevalent mixing rule is what we refer to as the conventional volume mixing rule, in which the refractive indices of AS and water are linearly averaged, weighted by their respective volume fractions in solution:

$$m_{\text{solution}} = f_{\text{AS}}^{\text{volume}} m_{\text{AS}} + (1 - f_{\text{AS}}^{\text{volume}}) m_{\text{H2O}}, \quad (1)$$

where m_{solution} is the refractive index of the solution, $f_{\text{AS}}^{\text{volume}}$ is the volume fraction of AS, m_{AS} is the refractive index of pure AS, and m_{H2O} is the refractive index of water. (The equation may be applied separately to the real part and to the imaginary part of the refractive index.)

In implementing Eq. (1), the real part of the refractive index of pure AS in the near-ultraviolet and visible is generally taken to be 1.52–1.55, the range reported by a number of historical and current references (e.g., Toon et al. 1976; Pettersson et al. 2004; Abo Riziq et al. 2007). This range, however, is based on measurements of AS in the dry solid (crystalline) state. In the aqueous state, the refractive index of the AS component (not including the water) may be different than that of solid AS. In addition, mixing rules, such as Eq. (1), are derived under the assumption of dilute solutions and are therefore not necessarily good approximations for more concentrated solutions (see, e.g., Sihvola 1996; Chýlek et al. 2000; Erlick 2006). These factors lead to differences between the refractive index of AS–water solutions calculated according to Eq. (1) and empirically derived refractive indices of AS–water solutions based on light scattering measurements, such as those presented in Weast et al. (1985, p. D-223), Stelson (1990), and Tang and Munkelwitz (1991, 1994). (See our Fig. 1; compare the blue solid curve against the black circles and the black solid curve.)

Consequently, radiative transfer models [such as those of Haywood et al. (1997), Liu et al. (2007), and Donner et al. (2011)] that employ the conventional volume mixing rule produce different estimates of the radiative forcing efficiency (RFE) of AS aerosols than models [e.g., Tang 1996; Schmidt et al. 2006; see ftp://ftp.giss.nasa.gov/pub/crmim/lacis/lacis_refrac.rhwmri.f (hereafter lacis.f) for the Fortan code created by A. A. Lacis for the National Aeronautics and Space Administration (NASA) Goddard Institute for Space Studies (GISS) general circulation model] that employ empirically derived refractive indices or models [such as those of Jacobson (2001) and Wang et al. (2008)] that employ the molar refraction mixing rule, in which the (empirically derived) molar refractions of AS and water are linearly averaged, weighted by their respective molar fractions in solution (see the black dashed curve in Fig. 1).

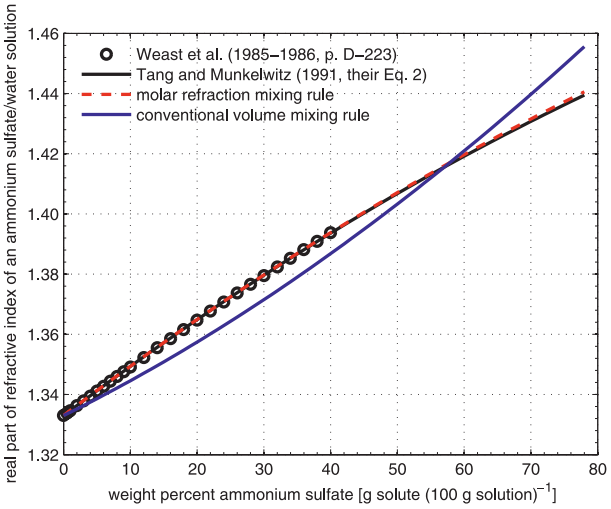

FIG. 1. Real part of the refractive index at 0.633-μm wavelength of a solution of AS with water as a function of the weight percentage of AS. The open black circles are data from Weast et al. (1985, p. D-223). The solid black line is the parametric formula of Tang and Munkelwitz [1991, their Eq. (2)] based on their empirical results for supersaturated solutions. The dashed red line is the molar refraction mixing rule. The solid blue line is the conventional volume mixing rule.

In the current study, we calculate the magnitude of such differences in the estimated RFE of AS aerosols in the solar wavelength range over a range of relative humidities at which AS can be found in solution with water in atmospheric aerosols (37.0%–99.9%). We perform two sets of calculations, one for aerosols consisting of an internal mixture of AS and water only, and one for aerosols consisting of an internal mixture of AS, water, and 2% black carbon by volume. The latter internal mixture is intended to be suggestive of sulfate-carbonaceous pollution aerosols (Bates et al. 2006). While such pollution aerosols often contain internally mixed organic carbon as well, because of the complexity of the influence of organic carbon on aerosol growth with humidity and additional uncertainties regarding properly representative refractive indices of organic carbon, in the current study, in a similar fashion to Donner et al. (2011), we exclude organic carbon from our internal mixture.

2. Methods

a. Calculating the single scattering parameters

All calculations are performed at the representative solar wavelength of 0.550 μm. The complex refractive

index of AS at 0.550 μm is taken to be $1.5298 + i1.00 \times 10^{-7}$ (lacis.f; Toon et al. 1976; Gosse et al. 1997) and that of water is taken to be $1.33457 + i1.958849 \times 10^{-9}$ (lacis.f). For the calculations employing the conventional volume mixing rule, Eq. (1) is used directly. For the calculations employing the empirically derived refractive indices, a version of lacis.f is used. In lacis.f, the empirical parametric formula in Tang and Munkelwitz [1991, their Eq. (2)] is used to obtain a ''refractive index proportionality factor'' or effective volume fraction in order to linearly interpolate the relative humidity dependence of the refractive index of the solution between the value for pure dry AS and the value for pure water.

For aerosols consisting of an internal mixture of AS, water, and 2% black carbon by volume, as in Donner et al. (2011), the refractive index of the aerosols containing black carbon are calculated using a further application of the conventional volume mixing rule:

$$m_{\text{solution with black carbon}} = 0.98 m_{\text{solution}} + 0.02 m_{\text{black carbon}}, \quad (2)$$

where $m_{\text{solution with black carbon}}$ is the refractive index of the internal mixture with black carbon, m_{solution} is the refractive index of the internal mixture without black carbon (calculated either using a prior application of the conventional volume mixing rule or using the version of lacis.f), and $m_{\text{black carbon}}$ is the refractive index of pure black carbon. The refractive index of pure black carbon is taken to be the index determined as optimal at 0.532-μm wavelength by Adler et al. (2010), namely $1.850 + i0.710$.

The dry aerosol size distribution is taken to be that of the water soluble aerosol component (described as consisting of sulfates, nitrates, and soluble organics) from Hess et al. (1998, their Table 1-C) (a lognormal size distribution with minimum radius = 0.005 μm, maximum radius = 20.0 μm, mode radius = 0.0212 μm, and standard deviation = 2.24 μm). Note that this size distribution is an average size distribution for the water soluble aerosol component in the troposphere.

In a similar fashion to Schmidt et al. (2006), the weight percentage (wt%) of AS in equilibrium with water at a given relative humidity is given by solving for the roots of the parametric relationship between water activity and weight percentage of AS presented in Tang [1996, his Eq. (6)], where the Kelvin effect due to the surface tension of the drop curvature is assumed negligible, and therefore the water activity is set equal to the relative humidity divided by 100%. The weight percentage of AS in equilibrium with water at a given relative humidity is then converted into a drop growth factor using Tang [1996, his Eq. (3)]:

$$\frac{D}{D_0} = \left(\frac{1}{f_{\text{AS}}^{\text{mass}}} \frac{\rho_0}{\rho_{\text{solution}}} \right)^{1/3}, \quad (3)$$

where D is the diameter of the aerosol at the current relative humidity, D_0 is the diameter of the drop at a reference relative humidity (taken to be any humidity less than or equal to approximately 35%), $f_{\text{AS}}^{\text{mass}}$ is the mass fraction of AS (the weight percentage divided by 100%) in solution at the current relative humidity, ρ_{solution} is the empirically determined density of the ammonium sulfate solution at the current relative humidity, given by Tang [1996, his Eq. (5)], and ρ_0 is the density of drop at the reference relative humidity at which the value for D_0 is set. The value for ρ_0 that gives the best match to the drop growth factor calculated using the thermodynamic model of Ming and Russell (2002) and to that used in Donner et al. (2011) is the value for dry crystalline AS given by Tang (1996, his Table 2)—that is, 1.76 g cm^{-3}. Since the Kelvin effect is assumed negligible, this same growth factor is applied to all sizes in the aerosol size distribution at a given relative humidity. Furthermore, this same growth factor is used whether the aerosols contain black carbon or not; that is, in a similar fashion to Liu et al. (2007) and to Donner et al. (2011), the growth of the aerosols with humidity is assumed to be influenced only by the AS.

For consistency with Eq. (3), in the current study, the volume fraction of AS used in conjunction with the conventional volume mixing rule is calculated from the mass fraction of AS via

$$f_{\text{AS}}^{\text{volume}} = f_{\text{AS}}^{\text{mass}} \frac{\rho_0}{\rho_{\text{solution}}}. \quad (4)$$

Equation (4) is equivalent to Brocos et al. [2003, their Eq. (10)]. Note that the conversion of mass fraction into volume fraction may also be achieved by an equation of the form [Brocos et al. 2003, their Eq. (8)]

$$f_{\text{AS}}^{\text{volume}} = \frac{\dfrac{f_{\text{AS}}^{\text{mass}}}{1 - f_{\text{AS}}^{\text{mass}}} \dfrac{\rho_{\text{H2O}}}{\rho_{\text{AS}}}}{1 + \dfrac{f_{\text{AS}}^{\text{mass}}}{1 - f_{\text{AS}}^{\text{mass}}} \dfrac{\rho_{\text{H2O}}}{\rho_{\text{AS}}}}, \quad (5)$$

where ρ_{H2O} is the density of water ($\sim$1.0 g cm^{-3}). However, in addition to being inconsistent with Eq. (3), Eq. (5) leads to an even larger difference in the calculated RFE between the conventional volume mixing rule and empirically derived refractive indices. Our choice of Eq. (4) therefore provides a more conservative estimate of the difference in RFE than Eq. (5) would.

Given the drop growth factor and the refractive index of the solution without or with black carbon, the single scattering albedo ϖ and asymmetry factor g of the aerosol size distribution at the given relative humidity are then calculated using the Mie scattering subroutine of Bohren and Huffman (1983, their appendix A).

b. Calculating the radiative forcing efficiency

Since our emphasis is on differences between forcing values, in a similar fashion to Anderson et al. (1999) and Dinar et al. (2008), we estimate the direct solar aerosol radiative forcing efficiency at the top of the atmosphere caused by a uniform, optically thin aerosol layer in the lower troposphere using Haywood and Shine [1995, their Eq. (3)]:

$$\mathrm{RFE} = \frac{\Delta F}{\tau} = SD(1 - A_{\mathrm{cld}})T_{\mathrm{atm}}^2(1 - R_{\mathrm{sfc}})^2 \times \left[2R_{\mathrm{sfc}}\frac{1 - \varpi}{(1-R_{\mathrm{sfc}})^2} - \beta\varpi\right], \quad (6)$$

where τ is the aerosol optical depth, S is the solar constant (set to 1370 W m^{-2}), D is the fractional day length (set to 0.5), A_{cld} is the fractional cloud cover (set to 0.61), T_{atm} is the solar atmospheric transmittance (set to 0.76), and R_{sfc} is the surface albedo (set to 0.15) (appropriate for a continental area) (Charlson et al. 1991; Randles et al. 2004). The parameter β is the average upscatter fraction (the fraction of scattered sunlight that is scattered into the upward hemisphere), which is a function of hemispheric backscatter fraction b, defined as the ratio of backscattering efficiency to total scattering efficiency. While in principle β and b can be calculated using the Mie scattering subroutine, for simplicity we follow Anderson et al. (1999) and use a simple functional relationship between β and b derived from the Henyey–Greenstein phase function:

$$\beta = 0.082 + 1.85b - 2.97b^2, \quad (7)$$

where, in terms of g (Wiscombe and Grams 1976; Bates et al. 2006),

$$b = \frac{1 - g^2}{2g}\left(\frac{1}{\sqrt{1 + g^2}} - \frac{1}{1 + g}\right). \quad (8)$$

ΔF is the change in net solar flux at the top of the atmosphere due to the presence of the aerosols $[(F^{\downarrow} - F^{\uparrow})_{\text{with aerosols}} - (F^{\downarrow} - F^{\uparrow})_{\text{without aerosols}}]$. Since $F^{\downarrow}$, the incident solar flux, is a constant, a negative value of RFE indicates an overall increase in upward scattering by the atmosphere due to the presence of aerosols, while a positive value of RFE indicates an overall decrease in upward scattering by the atmosphere due to the presence of the aerosols.

3. Results

The results of the RFE calculations are shown in Table 1 and in Fig. 2. For relative humidities less than around 66%, the conventional mixing rule produces a more negative RFE (equivalent to more upward scattering and hence potential cooling) than the empirically derived refractive indices, while for relative humidities greater than 66%, the conventional mixing rule produces a less negative RFE (equivalent to less upward scattering and hence potential warming) than the empirically derived refractive indices. The point of crossover from more negative RFE to less negative RFE at around 66% relative humidity in Fig. 2 corresponds to the weight percentage of AS at which the conventional volume mixing rule crosses over the empirically derived refractive indices in Fig. 1, namely 57–58 wt%. The aerosols cross from a higher refractive index with the conventional volume mixing rule than with the empirically derived refractive indices at high weight percentage AS to a lower refractive index with the conventional volume mixing rule than with the empirically derived refractive indices at low weight percentage AS. The higher refractive index with the conventional volume mixing rule at high weight percentage AS makes the aerosol more scattering than with the empirically derived refractive indices, and hence leads to an increase in upward scattering and a more negative RFE. The lower refractive index with the conventional volume mixing rule at low weight percentage AS makes the aerosol less scattering than with the empirically derived refractive indices, which leads to a decrease in upward scattering and a less negative RFE. These differences potentially lead to over/underestimation of the radiative properties of AS aerosols in climate models that use the conventional mixing rule.

Without black carbon, the difference in RFE is up to -0.42 W m^{-2} for relative humidities less than around 66% and up to 0.25 W m^{-2} for relative humidities greater than 66%, while with 2% black carbon by volume, the range of difference in RFE is up to -0.59 W m^{-2} for relative humidities less than around 66% and up to 0.30 W m^{-2} for relative humidities greater than 66%. Mathematically speaking, the range of difference is larger with black carbon than without, since with black carbon there is a difference in the single scattering albedo as well as in the asymmetry factor in Eq. (6). [Note that according to Eq. (6), for a nonabsorbing aerosol ($\varpi = 1$), a change in RFE is caused principally by a change in β, which in turn is caused by a change in g.] Physically

TABLE 1. Refractive index (RI), ϖ, g, and TOA RFE at 0.550-μm wavelength for AS aerosols as a function of RH, calculated with the conventional volume mixing rule (''volume'') and with the empirically derived parametric formula of Tang and Munkelwitz [1991, their Eq. (2)] (''empirical''), and using the dry aerosol size distribution of the water soluble component of the urban aerosol from Hess et al. (1998, Table 1-C).

RH (%)	RI volume[a]	RI empirical[a]	ϖ volume[b]	ϖ empirical[b]	g volume[b]	g empirical[b]	RFE volume[c] (W m^{-2})	RFE empirical[c] (W m^{-2})	RFE difference[c] (W m^{-2})
Without black carbon									
37.0	$1.462 + i6.587 \times 10^{-8}$	$1.444 + i5.689 \times 10^{-8}$	1.000	1.000	0.6527	0.6604	−26.76	−26.33	−0.42
40.0	$1.457 + i6.361 \times 10^{-8}$	$1.442 + i5.571 \times 10^{-8}$	1.000	1.000	0.6561	0.6630	−26.57	−26.19	−0.38
50.0	$1.443 + i5.619 \times 10^{-8}$	$1.433 + i5.163 \times 10^{-8}$	1.000	1.000	0.6665	0.6709	−26.00	−25.75	−0.24
60.0	$1.428 + i4.873 \times 10^{-8}$	$1.424 + i4.709 \times 10^{-8}$	1.000	1.000	0.6776	0.6791	−25.38	−25.30	−0.08
70.0	$1.412 + i4.088 \times 10^{-8}$	$1.414 + i4.179 \times 10^{-8}$	1.000	1.000	0.6908	0.6899	−24.66	−24.71	0.05
80.0	$1.395 + i3.206 \times 10^{-8}$	$1.400 + i3.506 \times 10^{-8}$	1.000	1.000	0.7076	0.7044	−23.74	−23.91	0.17
90.0	$1.372 + i2.084 \times 10^{-8}$	$1.380 + i2.498 \times 10^{-8}$	1.000	1.000	0.7301	0.7257	−22.50	−22.74	0.24
95.0	$1.356 + i1.283 \times 10^{-8}$	$1.363 + i1.640 \times 10^{-8}$	1.000	1.000	0.7541	0.7500	−21.20	−21.42	0.22
98.0	$1.343 + i6.412 \times 10^{-9}$	$1.347 + i8.360 \times 10^{-9}$	1.000	1.000	0.7776	0.7751	−19.94	−20.07	0.13
99.0	$1.339 + i4.119 \times 10^{-9}$	$1.341 + i5.162 \times 10^{-9}$	1.000	1.000	0.7862	0.7850	−19.48	−19.54	0.07
99.9	$1.335 + i2.165 \times 10^{-9}$	$1.335 + i2.273 \times 10^{-9}$	1.000	1.000	0.7952	0.7950	−19.00	−19.01	0.01
With 2% black carbon by volume									
37.0	$1.470 + i1.420 \times 10^{-2}$	$1.452 + i1.420 \times 10^{-2}$	0.9075	0.9044	0.6569	0.6642	−19.79	−19.20	−0.59
40.0	$1.465 + i1.420 \times 10^{-2}$	$1.450 + i1.420 \times 10^{-2}$	0.9071	0.9043	0.6600	0.6665	−19.61	−19.08	−0.52
50.0	$1.451 + i1.420 \times 10^{-2}$	$1.442 + i1.420 \times 10^{-2}$	0.9055	0.9039	0.6701	0.6741	−18.98	−18.68	−0.31
60.0	$1.436 + i1.420 \times 10^{-2}$	$1.433 + i1.420 \times 10^{-2}$	0.9037	0.9031	0.6816	0.6830	−18.28	−18.17	−0.11
70.0	$1.421 + i1.420 \times 10^{-2}$	$1.423 + i1.420 \times 10^{-2}$	0.9019	0.9023	0.6942	0.6934	−17.53	−17.59	0.06
80.0	$1.404 + i1.420 \times 10^{-2}$	$1.409 + i1.420 \times 10^{-2}$	0.9002	0.9013	0.7104	0.7076	−16.61	−16.83	0.22
90.0	$1.382 + i1.420 \times 10^{-2}$	$1.390 + i1.420 \times 10^{-2}$	0.8974	0.8989	0.7346	0.7307	−15.22	−15.52	0.29
95.0	$1.366 + i1.420 \times 10^{-2}$	$1.373 + i1.420 \times 10^{-2}$	0.8959	0.8971	0.7583	0.7545	−13.97	−14.24	0.27
98.0	$1.354 + i1.420 \times 10^{-2}$	$1.357 + i1.420 \times 10^{-2}$	0.8914	0.8920	0.7849	0.7827	−12.39	−12.53	0.14
99.0	$1.349 + i1.420 \times 10^{-2}$	$1.351 + i1.420 \times 10^{-2}$	0.8858	0.8860	0.7968	0.7956	−11.47	−11.54	0.07
99.9	$1.345 + i1.420 \times 10^{-2}$	$1.345 + i1.420 \times 10^{-2}$	0.8376	0.8376	0.8255	0.8255	−7.07	−7.07	0.00

[a] In a similar fashion to Tang and Munkelwitz (1991), the refractive indices are calculated to a precision of four significant figures, though other sources calculate refractive indices to even higher precision (see, e.g., Tang and Munkelwitz 1994; lacis.f).

[b] In a similar fashion to d'Almeida et al. (1991), the single scattering albedo and asymmetry factor are reported to a precision of four significant figures, although, as in most current models, the calculations are performed with double floating point precision (see lacis.f). The number of quadrature points chosen for integrating over the size distribution is that which gives the closest match to the values of single scattering albedo and asymmetry factor at 0.550-μm wavelength for dry water-soluble aerosols reported by d'Almeida et al. (1991, their Tables A.9 and A.10).

[c] Note that a lower precision in the refractive indices, single scattering parameters, and/or quadrature routine could lead to differences in the estimated RFE.

speaking, with black carbon the interaction between absorption and scattering amplifies the difference in RFE. However, we would expect that as the volume fraction of black carbon increases (not shown here), the difference in RFE would taper off, as increasingly strong absorption would subdue the scattering by the AS aerosols altogether. Both without and with black carbon, the difference in RFE approaches zero as the relative humidity approaches 100%, since at the highest relative humidities the amount of water in the internal mixture overwhelms the presence of the AS.

4. Conclusions

Using a simple model for calculating the RFE of an optically thin layer of aerosols and a reasonable description of the effect of humidity, we find that the difference between the conventional volume mixing rule and empirically derived refractive indices amounts to a modest difference in the direct solar RFE of AS aerosols at the top of the atmosphere at 0.550-μm wavelength and at relative humidities of 37%–99.9%, ranging from -0.42 W m^{-2} to 0.25 W m^{-2} without black carbon and from -0.59 W m^{-2} to 0.30 W m^{-2} with 2% black carbon by volume. For comparison, the range of RFE values at 0.550-μm wavelength for AS aerosols in Forster et al. (2007, their Table 2.4) is -8 to -32 W m^{-2}.

While the difference in the radiative forcing *efficiency* is modest, the difference in the absolute radiative forcing (RF) by AS aerosols (equal to the RFE times the aerosol optical depth) may be more significant.

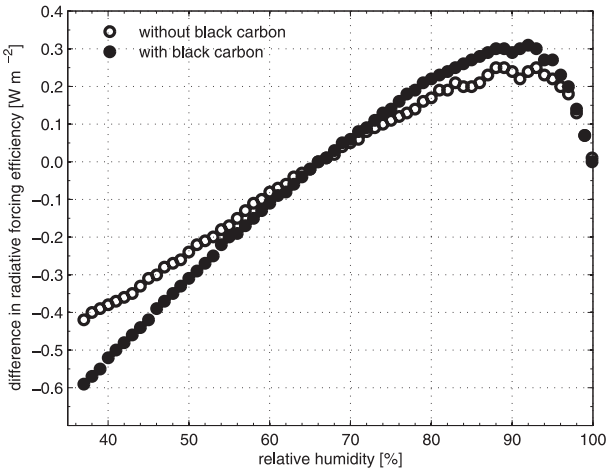

FIG. 2. Difference in top-of-the-atmosphere (TOA) RFE at 0.550-μm wavelength for AS aerosols as a function of RH calculated with the conventional volume mixing rule vs with the empirically derived parametric formula of Tang and Munkelwitz [1991, their Eq. (2)]. The open circles are calculations for internal mixtures of AS and water only. The filled circles are calculations for internal mixtures of AS, water, and 2% black carbon by volume.

To convert RFE to RF, we assume two different aerosol concentrations for the AS aerosol, again based on the tabulated characteristics of the water soluble aerosol component given by Hess et al. (1998). For average continental aerosol, we take an aerosol concentration of 7000 cm^{-3}, while for urban aerosol we take an aerosol concentration of 28 000 cm^{-3} (Hess et al. 1998, their Table 4). Assuming a 1-km aerosol layer depth, the 0.550-μm optical depth of the average continental AS aerosol ranges from 0.04 at 27% relative humidity to a nominal value of 0.07–0.08 at 80% relative humidity to 5.57–5.60 at 99.9% relative humidity. The corresponding difference in direct solar RF by average continental AS aerosols at the top of the atmosphere ranges from −0.06 to 0.15 W m^{-2} without black carbon and ranges from −0.06 to 0.12 W m^{-2} with 2% black carbon by volume. Assuming a 1-km aerosol layer depth, the 0.550-μm optical depth of the urban AS aerosol ranges from 0.14–0.16 at 27% relative humidity to a nominal value of 0.29–0.31 at 80% relative humidity to 22.27–22.40 at 99.9% relative humidity. The corresponding difference in direct solar RF by urban AS aerosols at the top of the atmosphere ranges from −0.26 to 0.62 W m^{-2} without black carbon and from −0.23 to 0.47 W m^{-2} with 2% black carbon by volume. Compare this to the range of estimated total aerosol direct RF presented by Forster et al. (2007), −0.9 to −0.1 W m^{-2}. In areas with a high concentration of urban and industrial pollution, such as northeastern China and northern India, where the nominal aerosol optical depth may be 0.5 or higher (e.g., Che et al. 2009; Vinoj et al. 2004), the difference in direct solar RF by AS aerosols would be correspondingly even higher. Therefore, the difference between the conventional volume mixing rule and empirically derived refractive indices may be an important one when investigating regional aerosol forcing. This suggests that models should employ the empirically derived refractive indices in order to obtain a more accurate estimation of the regional direct effect of AS aerosol.

A more thorough calculation of the difference between the conventional volume mixing rule and empirically derived refractive indices on the radiative forcing by AS aerosols may be obtained using the radiation component of a general circulation model and full offline microphysical and Mie scattering calculations of the effect of humidity, but we do not expect the order of magnitude of the effect to differ from our estimation here.

Acknowledgments. This work was support by the Israel Science Foundation Grants 1527/07 and 196/08. Y. R. acknowledges support from the Helen and Martin Kimmel Award for Innovative Investigation and the FP7-ENV-2010-265148-PEGASOS grant. We thank Ziv Moreno for conducting a preliminary literature search; Yi Ming and Huan Guo for providing details regarding the NOAA/GFDL and the University of Michigan radiative transfer models, respectively; and two anonymous reviewers for their very helpful comments.

REFERENCES

Abo Riziq, A., C. Erlick, E. Dinar, and Y. Rudich, 2007: Optical properties of absorbing and non-absorbing aerosols retrieved by cavity ring down (CRD) spectroscopy. *Atmos. Chem. Phys.,* **7,** 1523–1536.

Adler, G., A. Abo Riziq, C. Erlick, and Y. Rudich, 2010: Effect of intrinsic organic carbon on the optical properties of fresh diesel soot. *Proc. Natl. Acad. Sci. USA,* **107,** 6699–6704.

Anderson, T. L., D. S. Covert, J. D. Wheeler, J. M. Harris, K. D. Perry, B. E. Trost, D. J. Jaffe, and J. A. Ogren, 1999: Aerosol backscatter fraction and single scattering albedo: Measured values and uncertainties at a coastal station in the Pacific Northwest. *J. Geophys. Res.,* **104** (D21), 26 793–26 807.

Bates, T. S., and Coauthors, 2006: Aerosol direct radiative effects over the northwest Atlantic, northwest Pacific, and north Indian Oceans: Estimates based on in-situ chemical and optical measurements and chemical transport modeling. *Atmos. Chem. Phys.,* **6,** 1657–1732.

Bohren, C. F., and D. R. Huffman, 1983: *Absorption and Scattering of Light by Small Particles.* John Wiley and Sons, 530 pp.

Braban, C. F., and J. P. D. Abbatt, 2004: A study of the phase transition behavior of internally mixed ammonium sulfate–malonic acid aerosols. *Atmos. Chem. Phys.,* **4,** 1451–1459.

Brocos, P., Á. Piñeiro, R. Bravo, and A. Amigo, 2003: Refractive indices, molar volumes and molar refractions of binary liquid mixtures: Concepts and correlations. *Phys. Chem. Chem. Phys.,* **5,** 550–557.

Charlson, R. J., J. Langner, H. Rodhe, C. B. Leovy, and S. G. Warren, 1991: Perturbation of the Northern Hemisphere radiative balance by backscattering from anthropogenic sulfate aerosols. *Tellus,* **43A,** 152–163.

Che, H., and Coauthors, 2009: Instrument calibration and aerosol optical depth validation of the China Aerosol Remote Sensing Network. *J. Geophys. Res.,* **114,** D03206, doi:10.1029/2008JD011030.

Chýlek, P., G. Videen, D. J. W. Geldart, J. S. Dobbie, and H. C. W. Tso, 2000: Effective medium approximations for heterogeneous particles. *Light Scattering by Nonspherical Particles: Theory, Measurements, and Applications,* M. I. Mishchenko, J. W. Hovenier, and L. D. Travis, Eds., Academic Press, 273–308.

d'Almeida, G. A., P. Koepka, and E. P. Shettle, 1991: *Atmospheric Aerosols: Global Climatology and Radiative Characteristics*. A. Deepak, 561 pp.

Dinar, E., A. Abo Riziq, C. Spindler, C. Erlick, G. Kiss, and Y. Rudich, 2008: The complex refractive index of atmospheric and model humic-like substances (HULIS) retrieved by a cavity ring down aerosol spectrometer (CRD-AS). *Faraday Discuss.,* **137,** 279–295.

Donner, L. J., and Coauthors, 2011: The dynamical core, physical parameterizations, and basic simulation characteristics of the atmospheric component AM3 of the GFDL global coupled model CM3. *J. Climate,* **24,** 3484–3519.

Erlick, C., 2006: Effective refractive indices of water and sulfate drops containing absorbing inclusions. *J. Atmos. Sci.,* **63,** 754–763.

Forster, P., and Coauthors, 2007: Changes in atmospheric constituents and in radiative forcing. *Climate Change 2007: The Physical Science Basis,* S. Solomon et al., Eds., Cambridge University Press, 129–234.

Gosse, S. F., M. Wang, D. Labrie, and P. Chylek, 1997: Imaginary part of the refractive index of sulfates and nitrates in the 0.7–2.6-μm spectral region. *Appl. Opt.,* **36,** 3622–3634.

Hallquist, M., and Coauthors, 2009: The formation, properties and impact of secondary organic aerosol: Current and emerging issues. *Atmos. Chem. Phys.,* **9,** 5155–5236.

Haywood, J. M., and K. P. Shine, 1995: The effect of anthropogenic sulfate and soot aerosol on the clear sky planetary radiation budget. *Geophys. Res. Lett.,* **22,** 603–606.

——, D. L. Roberts, A. Slingo, J. M. Edwards, and K. P. Shine, 1997: General circulation model calculations of the direct radiative forcing by anthropogenic sulfate and fossil-fuel soot aerosol. *J. Climate,* **10,** 1562–1577.

Hess, M., P. Koepke, and I. Schult, 1998: Optical properties of aerosols and clouds: The software package OPAC. *Bull. Amer. Meteor. Soc.,* **79,** 831–844.

Jacobson, M. Z., 2001: Global direct radiative forcing due to multicomponent anthropogenic and natural aerosols. *J. Geophys. Res.,* **106,** 1551–1568.

Liu, X., J. E. Penner, B. Das, D. Bergmann, J. M. Rodriguez, S. Strahan, M. Wang, and Y. Feng, 2007: Uncertainties in global aerosol simulations: Assessment using three meteorological data sets. *J. Geophys. Res.,* **112,** D11212, doi:10.1029/2006JD008216.

Marcolli, C., and U. K. Krieger, 2006: Phase changes during hygroscopic cycles of mixed organic/inorganic model systems of tropospheric aerosols. *J. Phys. Chem.,* **110A,** 1881–1893.

——, B. P. Luo, and T. Peter, 2004: Mixing of the organic aerosol fractions: Liquids as the thermodynamically stable phases. *J. Phys. Chem.,* **108A,** 2216–2224.

Martin, S. T., J. C. Schlenker, A. Malinowski, H. M. Hung, and Y. Rudich, 2003: Crystallization of atmospheric sulfate–nitrate–ammonium particles. *Geophys. Res. Lett.,* **30,** 2102, doi:10.1029/2003GL017930.

Meyer, N. K., and Coauthors, 2009: Analysis of the hygroscopic and volatile properties of ammonium sulphate seeded and unseeded SOA particles. *Atmos. Chem. Phys.,* **9,** 721–732.

Mikhailov, E., S. Vlasenko, S. T. Martin, T. Koop, and U. Pöschl, 2009: Amorphous and crystalline aerosol particles interacting with water vapor: Conceptual framework and experimental evidence for restructuring, phase transitions, and kinetic limitations. *Atmos. Chem. Phys.,* **9,** 9491–9522.

Ming, Y., and L. M. Russell, 2002: Thermodynamic equilibrium of organic-electrolyte mixtures in aerosol particles. *AIChE J.,* **48,** 1331–1348.

Pettersson, A., E. R. Lovejoy, C. A. Brock, S. S. Brown, and A. R. Ravishankara, 2004: Measurement of aerosol optical extinction at 532 nm with pulsed cavity ring down spectroscopy. *J. Aerosol Sci.,* **35,** 995–1011.

Randles, C. A., L. M. Russell, and V. Ramaswamy, 2004: Hygroscopic and optical properties of organic sea salt aerosol and consequences for climate forcing. *Geophys. Res. Lett.,* **31,** L16108, doi:10.1029/2004GL020628.

Schlenker, J. C., A. Malinowski, S. T. Martin, H. M. Hung, and Y. Rudich, 2004: Crystals formed at 293 K by aqueous sulfate–nitrate–ammonium–proton aerosol particles. *J. Phys. Chem.,* **108A,** 9375–9385.

Schmidt, G. A., and Coauthors, 2006: Present-day atmospheric simulations using GISS ModelE: Comparison to in situ, satellite, and reanalysis data. *J. Climate,* **19,** 153–192.

Sihvola, A., 1996: *Electromagnetic Mixing Formulas and Applications*. The Institution of Electrical Engineers, 284 pp.

Stelson, A. W., 1990: Urban aerosol refractive index prediction by partial molar refraction approach. *Environ. Sci. Technol.,* **24,** 1676–1679.

Tang, I. N., 1996: Chemical and size effects of hygroscopic aerosols on light scattering coefficients. *J. Geophys. Res.,* **101** (D14), 19 245–19 250.

——, and H. R. Munkelwitz, 1991: Simultaneous determination of refractive index and density of an evaporating aqueous solution droplet. *Aerosol Sci. Technol.,* **15,** 201–207.

——, and ——, 1994: Water activities, densities, and refractive indices of aqueous sulfates and sodium nitrate droplets of atmospheric importance. *J. Geophys. Res.,* **99,** 18 801–18 808.

——, K. H. Fung, D. G. Imre, and H. R. Munkelwitz, 1995: Phase transformations and metastability of hygroscopic microparticles. *Aerosol Sci. Technol.,* **23,** 443–453.

Toon, O. B., H. B. Pollack, and B. N. Khare, 1976: The optical constants of several atmospheric aerosol species: Ammonium sulfate, aluminum oxide, and sodium chloride. *J. Geophys. Res.,* **81,** 5733–5748.

Vinoj, V., S. K. Satheesh, S. Suresh Babu, and K. Krishna Moorthy, 2004: Large aerosol optical depths observed at an urban location in southern India associated with rain-deficit summer monsoon season. *Ann. Geophys.,* **22,** 3073–3077.

Wang, J., D. J. Jacob, and S. T. Martin, 2008: Sensitivity of sulfate direct climate forcing to the hysteresis of particle phase transitions. *J. Geophys. Res.,* **113,** D11206, doi:10.1029/2007JD009368.

Weast, R. C., M. J. Astle, and W. H. Beyer, Eds., 1985: *CRC Handbook of Chemistry and Physics*. 66th ed. CRC Press, 2363 pp.

Weingartner, E., M. Gysel, and U. Baltensperger, 2002: Hygroscopicity of aerosol particles at low temperatures. 1. New low-temperature H-TDMA instrument: Setup and first applications. *Environ. Sci. Technol.,* **36,** 55–62.

Whitby, K. T., 1984: Physical and optical behavior of sulfate-nitrate aerosols in equilibrium with atmospheric water vapor, ammonia and nitric acid. *Hygroscopic Aerosols,* L. H. Ruhnke and A. Deepak, Eds., A. Deepak, 45–63.

Winkler, P., and C. Junge, 1972: The growth of atmospheric aerosol particles as a function of the relative humidity. I. Method and measurements at different locations. *J. Rech. Atmos.,* **6,** 617–638.

Wiscombe, W. J., and G. W. Grams, 1976: The backscattered fraction in two-stream approximations. *J. Atmos. Sci.,* **33,** 2440–2451.